Microfluid Nanofluid (2015) 19:9–18
DOI 10.1007/s10404-014-1542-4

RESEARCH PAPER

Direct, one-step molding of 3D-printed structures for convenient fabrication of truly 3D PDMS microfluidic chips

Ho Nam Chan · Yangfan Chen · Yiwei Shu · Yin Chen · Qian Tian · Hongkai Wu

Received: 23 September 2014 / Accepted: 30 December 2014 / Published online: 10 January 2015

Abstract In this work, we developed a convenient, one-step soft-lithographic-based molding technique for molding truly 3D microfluidic channels in polydimethylsiloxane (PDMS) by overcoming two grand challenges. We optimized the post-treatment conditions for 3D-printed resin structures to facilitate the use of them as masters for PDMS replica molding. What is more important, we demonstrated a novel method for single-step molding from 3D-printed microstructures to generate truly 3D microfluidic networks easily. With this technique, we fabricated some key, functional 3D microfluidic structures and components including a basket-weaving network, a 3D chaotic advective mixer and microfluidic peristaltic valves. Furthermore, an interesting "injection-on-demand" microfluidic device was also demonstrated. Our technique offers a simple, fast route to the fabrication of 3D microfluidic chips in a short time without clean-room facilities.

Keywords 3D printing · Soft lithography · One-step molding · 3D microfluidic chip · PDMS

1 Introduction

In the past two decades, microfluidics has seen an explosive growth to offer unique technological tools in various applications (Xiong et al. 2014). Microfluidic networks can be roughly grouped into two categories based on the connectivity of the channels. The first type is two dimensional (planar), i.e., all channels in the network can be arranged onto a 2D (planar) plane. In microfluidic systems, the channels may take different 3D geometries (e.g., mushroom-like vs. rectangular cross-section of the channel); strictly speaking, they are both considered as planar because topologically, the 3D geometries do not change the connectivity of the channels, and hence, they are equivalent (Fig. 1). However, because these 3D geometries require special fabrication method from normal rectangular 2D planar networks, we consider them as pseudo-3D system. The second type is truly 3D network, which consists crossover features (i.e., one channel goes over and one channel under). With the crossover features, the channels can pass by each other without connecting, which is impossible in 2D and pseudo-3D system (Wu et al. 2000; Anderson et al. 2000). The truly 3D microfluidic systems can offer complexities and functions that 2D system cannot. Examples include basket-weaving channel networks (Chiu et al. 2000; Martinez et al. 2008), peristaltic valve (Unger et al. 2000; Thorsen et al. 2002; Liu et al. 2003) and 3D chaotic advective mixer (Liu et al. 2000; Chen and Meiners 2004; Conlisk and O'Connor 2012).

For the fabrication of a 2D microfluidic network, the convenient way is to mold the microfeatures on a photolithographically defined master into the microchip material, followed by sealing the open channels with a flat substrate. Among all the molding methods, soft lithography is the most commonly used with polydimethylsiloxane (PDMS) as the chip material because of its simplicity, fast turnaround time and low cost. However, currently, truly 3D microfluidic networks cannot be formed by one-step molding technique because the molding material and the master structure will be interlocked with each other

Electronic supplementary material The online version of this article (doi:10.1007/s10404-014-1542-4) contains supplementary material, which is available to authorized users.

H. N. Chan · Y. Chen · Y. Shu · Y. Chen · Q. Tian · H. Wu (✉)
Department of Chemistry, Hong Kong University of Science and Technology, Clear Water Bay, Kowloon, Hong Kong, China
e-mail: chhkwu@ust.hk

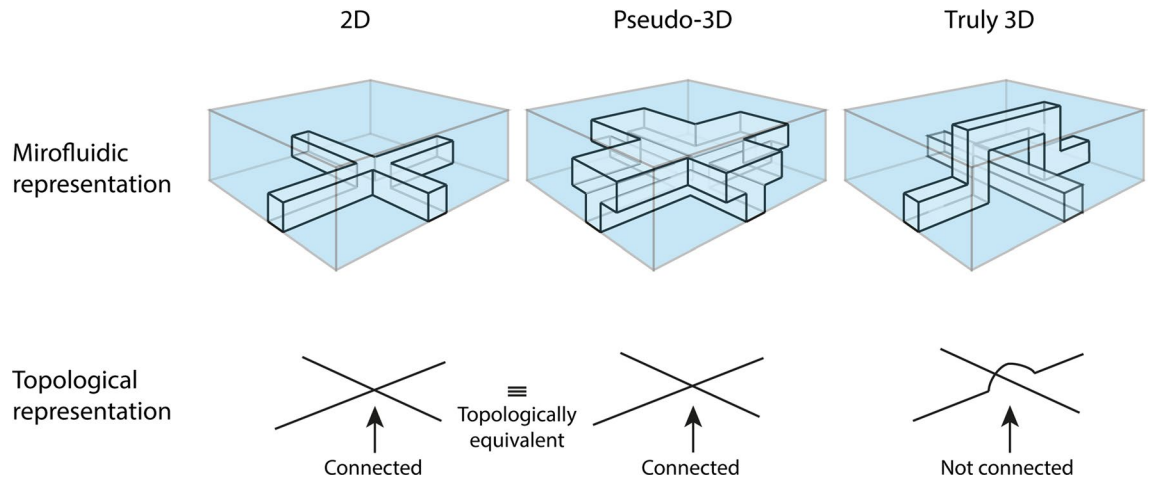

Fig. 1 Schematic representation of the three different types of microfluidic networks. Topologically, all microfluidic networks can be represented by *lines* regardless of their channel profile. For 2D network, all channels must be arranged on a plane regardless of their height, and they are rectangular due to the inherent nature of photolithography. Through the incorporation of specified fabrication technique, other channel profile can be constructed such as the mushroom-like structure, which *topographically* is a 3D channel. However, we classify this type of network as pseudo-3D because in terms of topology, they are equivalent to 2D network (see topological representation), which cannot form crossover features. For truly 3D networks, it consists of channels and crossover features, which are distinct from 2D and pseudo-3D network topologically

during the molding step. The straightforward strategy to fabricate them is by molding separate layers of the microfluidic network and stacking them to form the final structure, which is the layer-by-layer approach (Jo et al. 2000). This approach has shown its value in many representative applications such as highly integrated microfluidic chips (Thorsen et al. 2002; Liu et al. 2003; Kartalov and Quake 2004; Hong et al. 2004; Kartalov et al. 2006), single-cell analysis (Wheeler et al. 2003; Wu et al. 2004; Huang et al. 2007) and 3D chaotic advective mixer (Vijayendran et al. 2002; Chen and Meiners 2004; Xia et al. 2005). However, it is very time-consuming and labor intensive to align, stack and bond multiple thin PDMS layers well. Alternatively, two other strategies have been reported recently to fabricate 3D microfluidic chip. In the first, PDMS channel strips are weaved to form 3D microfluidic systems (Wu et al. 2003). Although it is simple in principle, the interconnections between channels in different strips cannot be generated. In the second, the chip material is molded against a sacrificial 3D template that can be removed after the chip material is solidified (Therriault et al. 2003; Verma et al. 2006; Wu et al. 2011; Esser-Kahn et al. 2011; Lee et al. 2012). However, the 3D template is not easily accessible at first hand, and each template can only be used once before it is destroyed or removed. Its wide application is greatly limited by the inherent serial nature of this approach.

With 3D printing as the readily expanding industry over the world that finds applications in many fields, the price of printer now comes to an affordable level for most research laboratories (Shallan et al. 2014). In recent years, some groups have proposed to 3D print microchip directly. This is a very attractive fabrication method mostly due to the ability to print complicated 3D microchip in a very short fabrication time with a high reproducibility because not much of the manual steps are involved. However, the choices of materials able to print three dimensionally are currently limited and show high contrast to the most common microchip material—PDMS. For instance, the 3D-printed reactors proposed by Cronin group are completely opaque, which hindered on-chip observation (Kitson et al. 2012, 2014). This problem also appears in the early work from Spence group, which designed a 3D-printed chip that can be coupled with cell culture inserts (Anderson et al. 2013). Later on, Spence, Breadmore and Folch group reported their chip designs and applications with a "transparent" 3D-printed chip material; however, none of the reported work showed transparency comparable to PDMS (Shallan et al. 2014; Au et al. 2014; Erkal et al. 2014; Lee et al. 2014; Chen et al. 2014). Furthermore, the biocompatibility of the 3D-printed chip is often questionable. Even though some resin does meet the biocompatibility standards, for example, the Somos® WaterShed XC 11122 used by Folch group, its gas permeability is still much poorer than PDMS, which prohibited long-term on-chip cell study (Au et al. 2014). Instead of using commercial available resin, recently, a group has investigated to 3D print PDMS directly (Femmer et al. 2014). But an orange dye was added in the resin in order to 3D print PDMS with an acceptable resolution, which turns out scarified the optical advantage of PDMS again. Furthermore,

even though the state-of-the-art commercial 3D printer can print features down to several tens of microns, it does not imply that a several tens of microns channel can be printed. This has been addressed in some literatures, and currently, only channels with dimension above 300 μm × 300 μm (width × height) can be printed (Shallan et al. 2014; Au et al. 2014).

Alternatively, using 3D-printing technology to replace the conventional clean-room-based photolithography to generate the master microstructures can offer several major advantages: (1) it does not require clean-room environment; (2) it can fabricate different channel profiles other than normally rectangular in photolithography; (3) it becomes very simple to fabricate structures with different heights, compared with the layer-by-layer strategy in photolithography; (4) suspended structures can be molded in one step without involving any alignment or sacrificial part; (5) chip material is no longer limited by the 3D printable resin, and it can be PDMS or other materials such as hydrogel to suit various microfluidic application (Ren et al. 2013). Recently, Comina et al. (2014) have reported using the Miicraft® 3D printer to print the soft-lithographic master for fabricating PDMS chips, bypassing the conventional clean room and wafer-based photolithographic step. In their technique, planar and pseudo-3D microfluidic channels can be successfully fabricated with single-step molding. However, for truly 3D microfluidic networks, they still relied on the layer-by-layer stacking. Moreover, because the 3D-printed material could interfere the curing reaction of PDMS (i.e., PDMS prepolymer in contact with the resin surface could not be fully cured), protective ink was required to coat on the 3D-printed master by airbrushing before molding in order to transfer the master pattern to PDMS. They claimed that this step requires practices to have an optimal finish; in addition, the bottom surface of suspended structures cannot be easily protected. Therefore, this extra step greatly offsets the convenience brought by 3D printing.

In this study, we developed a convenient soft-lithographic technique that allowed direct, *one-step* replica molding of printed 3D microstructures to form truly 3D microfluidic networks in PDMS without the airbrushing step. We investigated PDMS curing on 3D-printed master and found a more convenient post-treatment for the 3D-printed master, which solved problem of PDMS curing. In comparison, it is more challenging to directly mold truly 3D microstructures to form microfluidic networks with crossovers features in a single step. Recently, Fourkas et al. developed a membrane-assisted soft-lithographic method, which utilized an ultrathin membrane to prevent the PDMS from interlocking with the master that consists of a crossover structure so that the cured PDMS can be released from the master (LaFratta et al. 2006). However, it is very difficult to apply this technique for single-step molding in fabricating truly 3D microfluidic network because the generation of the thin membranes (~100 nm thick), the key element in the technique, requires expensive, sophisticated equipment. In our strategy, we adjusted the peeling direction and the geometry of 3D-printed master so that the interlocked PDMS at the crossover features can be ripped and released easily without the aid of thin membranes. The ripped PDMS part can be self-closed and healed by further curing afterward. The truly 3D microchannels with crossovers can thus be obtained with single-step molding. Our molding technique for truly 3D PDMS microfluidics is easy to perform and requires little special skill. We demonstrated the fabrication of some representative 3D functional microfluidic structures that are widely used, including a 3D chaotic advective mixer, basket-weaving microchannels and a peristaltic valve. A novel microfluidic device is also shown for injection-on-demand delivery of solutions. Compared with the conventional stacking method of fabricating 3D microfluidic chip, our proposed strategy eliminates the tedious repeating aligning and bonding steps of PDMS layers. Together with the advantages governed by 3D-printing which mentioned above, we believe that our strategy can facilitate the fabrication of both 2D and 3D chip and thus encourage investigation in 3D microfluidic applications.

2 Results and discussion

2.1 3D-printed master fabrication and its post-treatment

2.1.1 3D printing of master structure

The 3D printer used in this study was manufactured by Miicraft. Its *x*–*y* resolution is about 56 μm (450 ppi), while the *z* resolution is 50 μm. The printing mechanism and procedure were well described by Breadmore group (Shallan et al. 2014). In brief, the 3D models were firstly designed by CAD software (AutoCAD, Autodesk Inc., was used in this work). Afterward, the 3D-printing software sliced the 3D model in *z* direction to produce images representing each sliced layer of the model. The 3D printer reads the image and projected the corresponding UV pattern to the resin chamber. After a layer of resin had been cured, the substrate moved upward for 50 μm, which define the *z* resolution, to expose another layer of resin. By repeating the UV projection and the upward motion of the substrate, 3D model can be printed. In this study, all masters were printed with the following printing parameters: UV projection time for each single layer: 3.5 s; *z*-axis printing speed: 2 cm/h; *z*-axis resolution: 50 μm, unless mentioned specifically.

Each freshly printed master was soaked in industrial grade ethanol for 1 min and then further rinsed with ethanol to clean the unreacted resin. After air-dried, the masters

were UV post-cured for 600 s, as suggested by the manufacturer. It was found that a prolonged exposure to ethanol (e.g., 20 min) prior to the UV post-curing process could induce a higher chance of surface cracking in the heating treatment that will be discussed in the next section.

2.1.2 *Post-treatment of 3D-printed master enabling PDMS molding*

We found that the part of PDMS (RTV 615, GE Silicones, Wilton, CT, USA) prepolymer in contact with the 3D-printed objects cannot be polymerized into solid, which was also reported by others (Comina et al. 2014). The suspected reason is that the 3D-printed master is not fully reacted while the residual monomers and catalyst can inhibit the polymerization of PDMS. To remove the residual components in the 3D-printed master, a printed structure was treated with heat. The optimized procedures of this treatment are the following: (1) heat the 3D-printed master at 130 °C for 4 h in oven; (2) treat it with oxygen plasma at high power (Plasma cleaner, PDC-32 G, Harrick, USA) for 3 min; (3) coat its surface with fluorinated silane molecules by adding 10 μL trichloro(1H,1H,2H,2H-perfluoro-octyl) silane (Aldrich) in a desiccator under vacuum for 30 min. These steps serve for two purposes. Heating at 130 °C is an efficient way to get rid of the unreacted additives and monomers inside the printed master. Oxygen plasma treatment followed by silanization is for coating a monolayer of fluorinated molecules on the 3D-printed master to prevent PDMS from sticking to the master. Therefore, cured PDMS can be peeled off easily. Without the surface treatment, PDMS can be fully cured on the 3D-printed master; however, PDMS would adhere to the master adhere strongly so that PDMS would be torn off from the bulk and left on the master during the releasing step.

The most important parameters in the treatment are the heating temperature and time. Although heating at a higher temperature can shorten the heating time, heating at 150 °C or above could lead to obvious generation of cracks on the master surface. Our experiment results revealed that the optimal heating temperature is 130 °C. Because at this temperature, the required heating time for the master is at the order of few hours, and also the chance of generating undesired cracks is small. In Fig. 2, we showed the effect of heating time on the molding at 130 °C (from 1 to 4 h). For the control, which was not heated but still underwent the oxygen plasma and silanization treatment, the surface of PDMS contacting with the master was still in sticky and

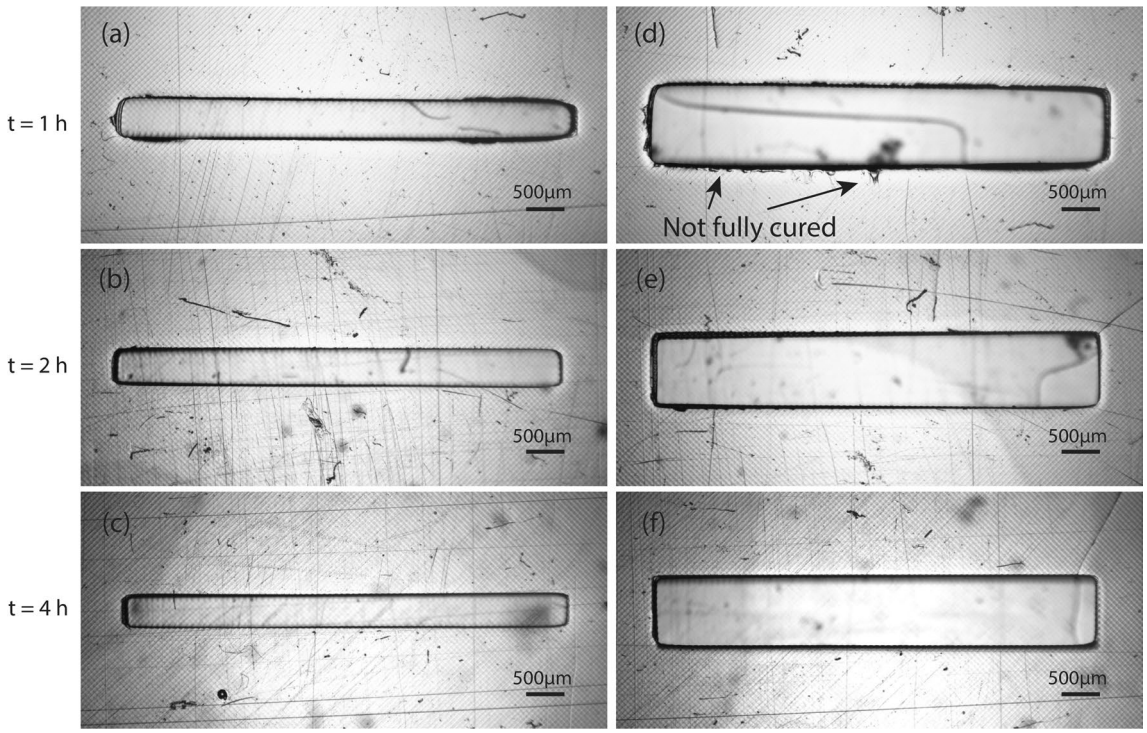

Fig. 2 Images of PDMS after releasing from the 3D-printed master. Each master was heated with the time indicated on *left* at 130 °C and treated with oxygen plasma and silanization. The images were focused on the contact surface between PDMS and master. **a–c** Images of molded PDMS channel (width and depth were 500 μm). PDMS was well cured for the 2-h heated master. **d–f** Images of molded PDMS channel (width and depth were 1 mm). For **d**, defects of the PDMS mold are indicated by *arrows*. The optimal result was obtained for the 4-h heated master

viscous liquid state (images not shown because none of the master features can be transferred to the PDMS). With increasing the heating duration of master gradually, we could observe that the soft-lithographic resolution goes better. For the 500-μm-wide channel, heating for 2 h gave an excellent molding result (Fig. 2b). As expected, larger master features need more time in the heating step to achieve excellent molding (Fig. 2f).

If a user does not demand immediate testing of the design, heating at 120 °C overnight is a good option to ensure the masters are well heated without generating cracks on the surface of the master. In the case that the master is under heated and PDMS does not cure well on the master, the master can be further heated in an oven for a proper time. Recasting PDMS prepolymer on this master again can also give excellent molding result. All of the 3D-printed masters described below were treated with these procedures.

2.2 Single-step molding for truly 3D microfluidic networks

Our strategy to mold truly 3D microfluidic networks with single-step molding is illustrated in Fig. 3a. As the cured PDMS and the master with crossover features are interlocked, peeling off the PDMS from the master will generate

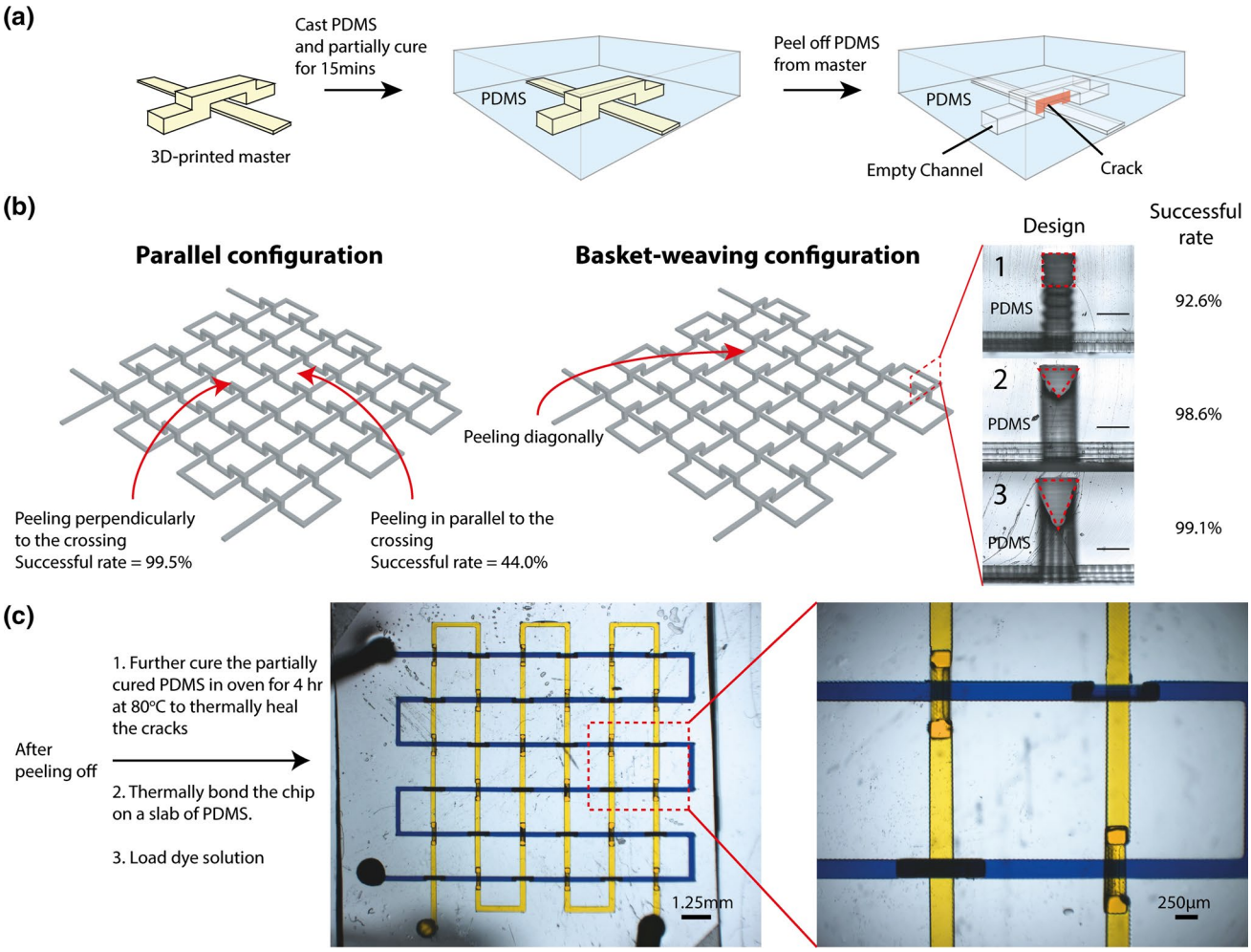

Fig. 3 Single-step molding for truly 3D microfluidic chips. **a** Schematic representation of fabricating a crossover features in one soft-lithographic step. The crack generated under the crossover feature is shown in *red*. **b** Investigation of the peeling direction and the influence of the crossover features profile on the peeling successful rate. Successful rate is defined as total number of crossover features successfully replicated/total number of crossover features. Designs *1–3* are the cross-section image of the molded crossover feature in PDMS. For the parallel configuration, only rectangular crossover profile was examined (design *1*, the *red dashed region* depicts the rectangular profile of the crossover feature). For basket-weaving configuration, both *rectangular* (design *1*) and *triangular* (design *2* and *3*, see *red dashed region*) crossover profile are examined. All peeling experiments were repeated for six times. *Scale bar* 250 μm. **c** Image of the permanently healed 3D chip (basket-weaving configuration with design *2*) loaded with yellow and blue dye solution. The yellow and blue streams are independent to each other, and no mixing or leakage was observed. *Right* magnified image of the *dash line* depicted region (color figure online)

a crack in the PDMS under the crossover features; as a result, the PDMS replica can be released from the master through the crack. To investigate the reproducibility of this approach, we designed a chip with 36 crossover features as shown in Fig. 3b. Such crossover features were arranged in two configurations, parallel and basket weaving.

Parallel configuration with rectangular crossover profile (i.e., the cross-section of the crossover feature is rectangular) is the simplest one, and this model was used to investigate the effect of peeling direction on the successful rate of this approach. All the peeling actions were done with bare hands without any tools, and the successful rate was defined as total number of crossover features successfully replicated/total number of crossover features. Two peeling direction was investigated, and the PDMS used in this section is 10:1 (A:B ratio) and partially cured for 15 min under 80 °C in an oven before peeling. Firstly, the PDMS was peeled off with a direction perpendicular to the orientation of the crossover features (Fig. 3b). After six times of trial, a total of 216 (36 × 6) crossover features were tested, and we found that the successful peeling rate of each individual crossover was 99.5 %. However, the successful rate of peeling the PDMS with a direction parallel to the crossover feature was dropped dramatically to 44.0 % (Fig. 3b). This is because, when it was peeled off perpendicularly, only one *edge* of the rectangular master exerted ripping force to the PDMS; as a result, a crack could be generated starting from that edges (Fig. S-1a). In contrast, peeling in parallel with the crossover allowed the ripping force exerted from the bottom *face* of the rectangular crossover features to the PDMS, which had a high probability to have two cracks generated simultaneously (Fig. S-1b). In other words, a piece of PDMS has a high chance to be torn off from the bulk body when we peel it off in parallel with the crossover features (Fig. S-1c, d).

For a technique to mold any truly 3D microfluidic channel network, it should not be limited by the configurations of the crossover features. Therefore, we tested our approach in the basket-weaving configuration (Fig. 3b), which can represent any truly 3D microfluidic chip topologically (Anderson et al. 2000). Suggested from our experimental result, peeling in parallel with any of the crossovers features decreases our successful rate since two cracks tended to be generated simultaneously with rectangular crossover profile. Thus, we peeled the chip off diagonally to avoid any parallel peeling. Same as before, the peeling experiment was repeated six times, and the successful rate was found to be 92.6 %. With this rate, the probability to fabricate a chip with 9 crossover features perfectly is estimated to be 50 % that is still too low for our approach to be applicable. Hence, in order to improve the successful rate, the basket-weaving configuration was tested again with triangular crossover profile (design 2, 3 in Fig. 3b). With the triangular features, the ripping force exerted to the PDMS will be confined at the bottom edges of the crossover no matter which peeling direction was chosen. As expected, the successful rate was increased to 98.6 % with design 2 and 99.1 % with design 3, which the probability to fabricate a chip containing 9 crossover perfectly increased to 92.2 %. To further illustrate the simplicity of this approach, we had taken a video showing the actual peeling action for molding the basket-weaving networks (design 2) in one-step (video S-1). In fact, the design of the crossover is not limited to only triangular profile; any design that have a single edge on the bottom (e.g., rhomboid, circular, 45° twisted rectangular profile) of the crossover master can be peeled off with a good successful rate in principle. Note that with 3D printing, all of these profiles, which are believed to be difficult to fabricate with traditional clean-room-based photolithography, can be generated easily by preparing a proper CAD file.

After released from the master, the PDMS crack will be self-closed due to its elasticity and self-adhesive properties. As we peeled the PDMS off under its partially cured state, we could permanently seal the crack by further thermal curing. This strategy is exactly same as the partially cured PDMS bonding technique commonly used in the field, which was proved to have a very strong bonding strength (370–680 kPa) (Eddings et al. 2008). To show that the 3D chip fabricated by this approach was free from leakage, a peeled off PDMS with basket-weaving channel networks (design 2) was chosen to make as a chip. As shown in Fig. 3c, the peeled off PDMS was firstly heated in an 80 °C oven for 4 h to permanently heal the cracks. Afterward, it was bonded with another slab of PDMS thermally. Finally, a yellow and blue dye solution was loaded into the channel. It was observed that the two sets of channels are independent to each other without leakage or mixing at all. This approach provides a simple solution for researchers to fabricated 3D microfluidic chip without any repeated bonding and alignment even without the clean-room facilities. As the complexity of chip keeps increasing with more sophisticated tasks, such 3D configuration allows researchers to transport different stream of fluid easily. Our technique saves time, efforts and costs to fabricate 3D microfluidics system and, hence, making fabrication no longer a huge barrier for researchers to take microfluidics as a tool in various studies and applications.

2.3 Fabrication of functional 3D microfluidic chips with single-step molding

2.3.1 3D chaotic advective mixer

3D chaotic advective mixer, which was introduced by Beebe et al., is an important microfluidic tool to facilitate fluidic mixing in low Reynolds number systems (Liu et al.

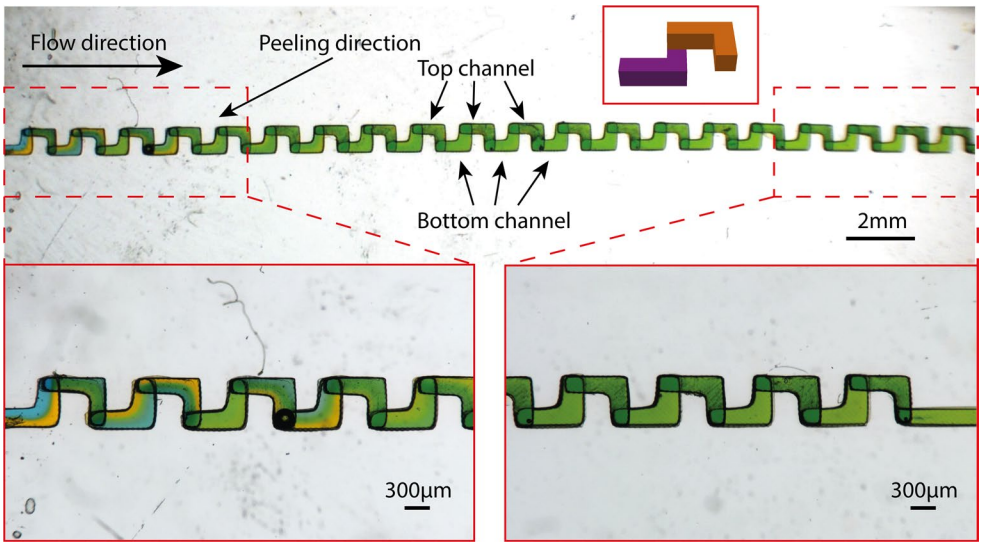

Fig. 4 Image of "L-shape" 3D chaotic advective mixer flowed with *blue* and *yellow* dye solution. The flow direction is from *left* to *right*. (*Inset*) *top* schematic representation of the repeating unit of "L-shape" 3D microfluidic mixer. *Top* channel is labeled as *orange*, while *bottom* channel as *purple*. *Left* magnified image of the beginning part of the mixer. Laminar flow was seen clearly. *Right* magnified image of the ending part of the mixer. The two fluid streams were indistinguishable with each other (color figure online)

2000). Because its structure is truly 3D, it required multiple molding, bonding and aligning steps to fabricate with conventional technique. However, in our demonstration, we were able to mold this structure in a single step directly. The "L-shape" mixer was selected from the work of Beebe et al. (Jo et al. 2000). Here, the fabricated PDMS 3D chaotic advective mixer had an upper and lower layer of channels with 300 μm in both width and height (Fig. 4). We fabricated this chip by casting 10:1 PDMS prepolymer on the 3D-printed master followed by partially curing for 15 min at 80 °C. Next, we peeled off the PDMS from the master with a direction as shown in Fig. 4. As peeling off with that direction, the ripping force is exerted from the corner of the upper crossover features to the PDMS. Hence, even with rectangular crossover profile, such 3D mixer with 22 crossover features can be peeled off successfully. After further curing in the oven for 4 h, the cracks were healed permanently. The 3D channel was sealed with a flat PDMS piece. To test this single-step molded 3D mixer, blue and yellow dye solution was introduced to the mixer. As indicated, the fluid flowed from left to right with a flow rate of 1 μL/min. The inset of Fig. 4 shows that the two fluid streams were laminar at the beginning and mixed quickly. At the end, the two fluid streams were indistinguishable with each other, which proved the intended function of the mixer.

2.3.2 *Peristaltic valve*

A more widely used 3D microfluidic device is a peristaltic valve that is made with multilayer soft lithography. This component is an excellent tool to manipulate fluid on-chip, which leads to the realization of many impressive microfluidic applications such as highly integrated microfluidic chip (Thorsen et al. 2002; Liu et al. 2003; Kartalov and Quake 2004; Hong et al. 2004; Kartalov et al. 2006), single-cell analysis (Wheeler et al. 2003; Wu et al. 2004; Huang et al. 2007), protein crystallization (Hansen et al. 2002) and cell sorting (Fu et al. 2002). In the peristaltic valve, a thin PDMS layer is sandwiched between a control channel and a flow channel; pressure in the control channel can deform the PDMS membrane to close or open the flow channel beneath. For its fabrication, three PDMS layers are required to be molded separately and bonded together with careful alignment.

With our technique, only a single step of molding is required to make the 3D structure of this peristaltic valve without any bonding with alignment. Subsequently, this PDMS microchannel structure was sealed by bonding with a PDMS slab or a glass slide through oxygen plasma treatment. The cross-section of the fabricated PDMS chip is shown in Fig. 5a. The top layer is the control channel, while the bottom layer is the flow channel with 43 μm in height. The PDMS membrane in between is ~100 μm thick. In Fig. 5b, the flow channel was loaded with a solution of 1-μm-diameter fluorescent microbeads, and the control channel was dead end loaded with water. After applying pressure (~140 kPa) to the control channel, the thin membrane was pushed downward to regulate and close the flow channel beneath (Fig. 5c). In Fig. 5d, a solution of fluorescent microbeads was injected continuously into the flow channel with a flow rate of 0.4 μL/min (Fig. 5d). We applied pressure of 140 kPa with a frequency of 0.5 Hz to the control channel to close and open the valve periodically (video S-2). Figure 5e shows an image of the functioning valve when the pressure was applied. It can be clearly seen that the microbeads stopped in position immediately when the valve was closed and flowed along the channel when the valve was opened.

The Miicraft® 3D printer is based on UV stereolithography with resolution around 50 μm in the z direction. That is,

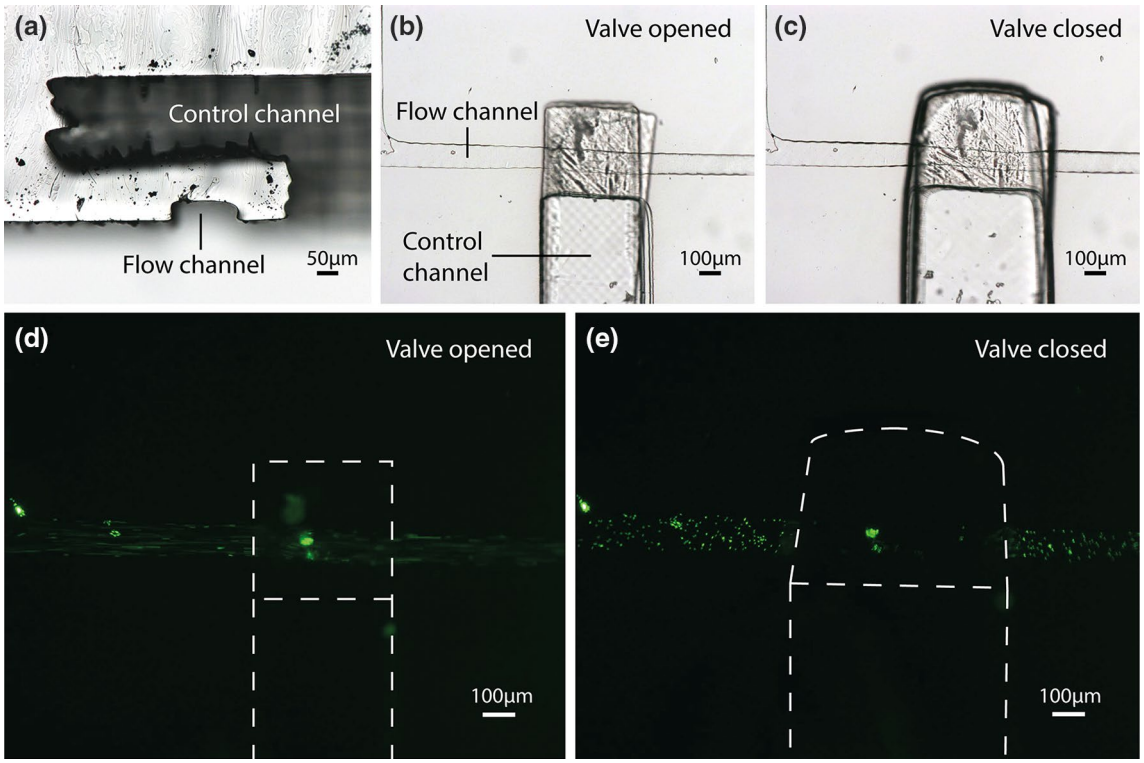

Fig. 5 One-step molded peristaltic valve. **a** Image of the cross-section of the PDMS peristaltic valve. **b** *Top* view of the PDMS peristaltic valve. Flow channel was loaded with fluorescent microbeads solution. Control channel was dead end loaded with water. **c** Pressure (140 kPa) was applied to the control channel. Channel was expanded due to the applied pressure. Fluorescent images of the chip with **d** valve opened, **e** valve closed. Exposure time of both image is 300 ms. The *white dashed lines* indicate the position of the valve

resin structures can have features with the smallest dimension of 50 μm in the z direction. However, the smallest gap in the z direction is ~100 μm because of the photolithographic nature of the 3D-printing technique [i.e., the resin in the gap is influenced by the residual light that is used to cure the resin layers on top of it, which is also reported by others (Shallan et al. 2014; Au et al. 2014)]. Also because of the limited resolution of current 3D printer, channels with dimension <100 μm can only have a rectangular profile, which requires higher pressure to close the valve completely compared to channels with rounded profile. In order to avoid high pressure, which can cause chip bursting and inlet leakage, we used soft PDMS with 25:1 prepolymer ratio instead of the normal 10:1 ratio. With a 3D printer with higher resolution, we could make a peristaltic valve with a thinner sandwiched membrane and a rounded flow channel that could be controlled with smaller pressure.

2.3.3 Injection-on-demand 3D microfluidic devices

Although the crack formed during the single-step molding normally needs to be permanently sealed afterward, we can choose to heal the crack reversibly (i.e., healing by self-adhesive force solely) for some unusual applications. Here, we applied the self-adhesive PDMS cracks to function as an injection-on-demand microfluidic device. The design is shown in Fig. 6a. In this example, the crossover features were designed to have a 45° rotated rectangular profile to confine that the crack was generated just under the features with the same idea stated in Sect. 2.2 (Fig. 6b). This structure was also selected to show that the 3D printing technology could fabricate a channel profile that was believed to be hard to achieve with the standard photolithographic technique (e.g., channels with circular, triangular, rhomboid, hexagonal cross-sections). The PDMS (10:1) used in this experiment was fully cured (4 h at 80 °C) prior to peeling off from the master; therefore, the crack cannot be irreversibly healed afterward by further thermal curing. Then, the chip was bonded to another slab of PDMS through oxygen plasma bonding technique. The PDMS in between top and bottom channel was ~200 μm thick. Once a gas pressure pulse (5.8 kPa for 0.04 s) was applied to the top channel (blue dye solution filled), the solution was injected to the bottom channel (water flowed continuously at 4 μL/min) through the crack (Fig. 6c; video S-2). For this chip, the threshold pressure of injection is 5.5 kPa. Below this pressure, the solution did not leak from the top channel to the bottom channel even supplying such pressure continuously. This result also indicates that the

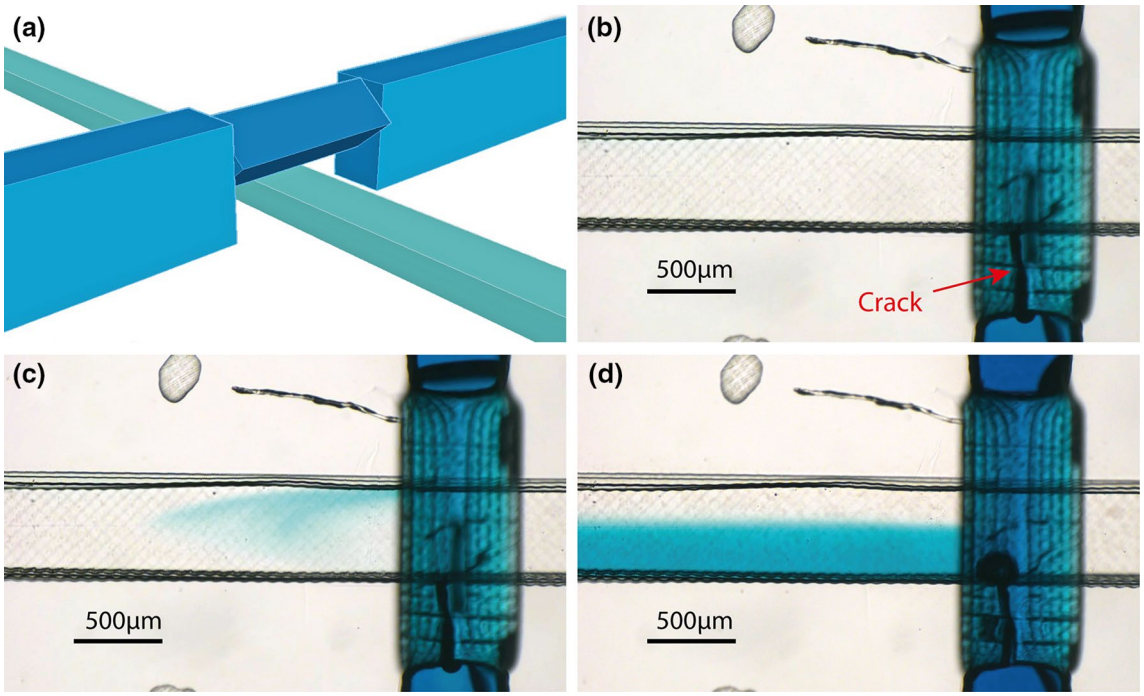

Fig. 6 Injection-on-demand 3D microfluidic device. **a** Part of the CAD of the 3D-printed master intended to show the 45° rotated rectangular crossover feature. **b** Image of the chip loaded with blue dye solution and water on the *top* and *bottom* channel, respectively, without applying any gas pressure. **c** Image of pulse injection with pressure applied at the *top* channel. The amplitude of the applied pressure pulse was 5.8 kPa that lasted for 0.04 s. Parabolic flow pattern could be observed, as the *bottom* channel flow was pressure driven. **d** Image of continuous injection. Both channels was flowed at 10 μL/min, and laminar flow was observed

barely self-adhesive strength of ~200-μm-thick 10:1 PDMS can withstand a maximum pressure of 5.5 kPa, which is acceptable for common microfluidic applications that do not demand high-pressure flow. Next, the outlet of the top channel was blocked, and both the blue solution and water were flowed with a rate of 10 μL/min by syringe pump to show a continuous injection with laminar flow (Fig. 6d). These demonstrated injection modes are proved to be useful for some applications (Cannon et al. 2003; Mosadegh et al. 2010).

3 Conclusion

The 3D printing as an emerging technology has recently shown its great potentials in microfluidics for convenient fabrication of various microchips. In this report, we have demonstrated two contributions in incorporating 3D printing into microfluidic fabrication. In one, we showed the "heating–plasma–silanization" treatment of printed masters as an easy way for molding the masters into PDMS. For truly 3D structures, we developed a convenient and efficient method for directly molding them into PDMS in a single step. This method greatly facilitates the fabrication of 3D microfluidic and can be performed easily as showed in video S-1. Some typical examples of widely used 3D microfluidic devices were demonstrated with this method. A novel injection-on-demand microfluidic device was also shown by taking the advantages of the cracks formed during the single-step molding process. We expect that the fabrication advancements of 3D microfluidic systems will benefit many researchers in this field by simplifying the fabrication process, shortening the process time and avoiding clean-room facilities. We also believe that because of its convenience, our method will promote investigations on applications with more 3D microfluidic structures.

Acknowledgments The authors are grateful for the funding provided by Hong Kong Research Grants Council (#605210, #604712 and CUHK4/CRF/12G).

References

Anderson JR, Chiu DT, Jackman RJ et al (2000) Fabrication of topologically complex three-dimensional microfluidic systems in PDMS by rapid prototyping. Anal Chem 72:3158–3164

Anderson KB, Lockwood SY, Martin RS, Spence DM (2013) A 3D printed fluidic device that enables integrated features. Anal Chem 85:5622–5626. doi:10.1021/ac4009594

Au AK, Lee W, Folch A (2014) Mail-order microfluidics: evaluation of stereolithography for the production of microfluidic devices. Lab Chip 14:1294–1301. doi:10.1039/c3lc51360b

Cannon DM, Kuo T, Bohn PW, Sweedler JV (2003) Nanocapillary array interconnects for gated analyte injections and electrophoretic separations in multilayer microfluidic architectures. Anal Chem 75:2224–2230. doi:10.1021/ac020629f

Chen H, Meiners J-C (2004) Topologic mixing on a microfluidic chip. Appl Phys Lett 84:2193–2195. doi:10.1063/1.1686895

Chen C, Wang Y, Lockwood SY, Spence DM (2014) 3D-printed fluidic devices enable quantitative evaluation of blood components in modified storage solutions for use in transfusion medicine. Analyst 139:3219–3226. doi:10.1039/c3an02357e

Chiu DT, Jeon NL, Huang S et al (2000) Patterned deposition of cells and proteins onto surfaces by using three-dimensional microfluidic systems. Proc Natl Acad Sci USA 97:2408–2413. doi:10.1073/pnas.040562297

Comina G, Suska A, Filippini D (2014) PDMS lab-on-a-chip fabrication using 3D printed templates. Lab Chip 14:424–430. doi:10.1039/c3lc50956g

Conlisk K, O'Connor GM (2012) Analysis of passive microfluidic mixers incorporating 2D and 3D baffle geometries fabricated using an excimer laser. Microfluid Nanofluidics 12:941–951. doi:10.1007/s10404-011-0928-9

Eddings MA, Johnson MA, Gale BK (2008) Determining the optimal PDMS–PDMS bonding technique for microfluidic devices. J Micromech Microeng 18:067001. doi:10.1088/0960-1317/18/6/067001

Erkal JL, Selimovic A, Gross BC et al (2014) 3D printed microfluidic devices with integrated versatile and reusable electrodes. Lab Chip. doi:10.1039/c4lc00171k

Esser-Kahn AP, Thakre PR, Dong H et al (2011) Three-dimensional microvascular fiber-reinforced composites. Adv Mater 23:3654–3658. doi:10.1002/adma.201100933

Femmer T, Kuehne AJC, Wessling M (2014) Print your own membrane: direct rapid prototyping of polydimethylsiloxane. Lab Chip 14:2610–2613. doi:10.1039/c4lc00320a

Fu AY, Chou H-P, Spence C et al (2002) An integrated microfabricated cell sorter. Anal Chem 74:2451–2457. doi:10.1021/ac0255330

Hansen CL, Skordalakes E, Berger JM, Quake SR (2002) A robust and scalable microfluidic metering method that allows protein crystal growth by free interface diffusion. Proc Natl Acad Sci USA 99:16531–16536. doi:10.1073/pnas.262485199

Hong JW, Studer V, Hang G et al (2004) A nanoliter-scale nucleic acid processor with parallel architecture. Nat Biotechnol 22:435–439. doi:10.1038/nbt951

Huang B, Wu H, Bhaya D et al (2007) Counting low-copy number proteins in a single cell. Science 315:81–84. doi:10.1126/science.1133992

Jo B-H, Van Lerberghe LM, Motsegood KM, Beebe DJ (2000) Three-dimensional micro-channel fabrication in polydimethylsiloxane (PDMS) elastomer. Microelectromech Syst J 9:76–81. doi:10.1109/84.825780

Kartalov EP, Quake SR (2004) Microfluidic device reads up to four consecutive base pairs in DNA sequencing-by-synthesis. Nucleic Acids Res 32:2873–2879. doi:10.1093/nar/gkh613

Kartalov E, Zhong J, Scherer A et al (2006) High-throughput multi-antigen microfluidic fluorescence immunoassays. Biotechniques 40:85–90. doi:10.2144/000112071

Kitson PJ, Rosnes MH, Sans V et al (2012) Configurable 3D-Printed millifluidic and microfluidic "lab on a chip" reactionware devices. Lab Chip 12:3267–3271. doi:10.1039/c2lc40761b

Kitson PJ, Marshall RJ, Long D et al (2014) 3D printed high-throughput hydrothermal reactionware for discovery, optimization, and scale-up. Angew Chem Int Ed Engl 12723–12728. doi:10.1002/anie.201402654

LaFratta CN, Li L, Fourkas JT (2006) Soft-lithographic replication of 3D microstructures with closed loops. Proc Natl Acad Sci USA 103:8589–8594. doi:10.1073/pnas.0603247103

Lee J, Paek J, Kim J (2012) Sucrose-based fabrication of 3D-networked, cylindrical microfluidic channels for rapid prototyping of lab-on-a-chip and vaso-mimetic devices. Lab Chip 12:2638–2642. doi:10.1039/c2lc40267j

Lee W, Kwon D, Chung B et al (2014) Ultrarapid detection of pathogenic bacteria using a 3D immunomagnetic flow assay. Anal Chem 86:6683–6688. doi:10.1021/ac501436d

Liu RH, Stremler MA, Sharp KV et al (2000) Passive mixing in a three-dimensional serpentine microchannel. J Microelectromech Syst 9:190–197. doi:10.1109/84.846699

Liu J, Hansen C, Quake SR (2003) Solving the "world-to-chip" interface problem with a microfluidic matrix. Anal Chem 75:4718–4723

Martinez AW, Phillips ST, Whitesides GM (2008) Three-dimensional microfluidic devices fabricated in layered paper and tape. Proc Natl Acad Sci USA 105:19606–19611. doi:10.1073/pnas.0810903105

Mosadegh B, Kuo C-H, Tung Y-C et al (2010) Integrated elastomeric components for autonomous regulation of sequential and oscillatory flow switching in microfluidic devices. Nat Phys 6:433–437. doi:10.1038/nphys1637

Ren K, Zhou J, Wu H (2013) Materials for microfluidic chip fabrication. Acc Chem Res 46:2396–2406. doi:10.1021/ar300314s

Shallan AI, Smejkal P, Corban M et al (2014) Cost-effective three-dimensional printing of visibly transparent microchips within minutes. Anal Chem 86:3124–3130. doi:10.1021/ac4041857

Therriault D, White SR, Lewis JA (2003) Chaotic mixing in three-dimensional microvascular networks fabricated by direct-write assembly. Nat Mater 2:265–271. doi:10.1038/nmat863

Thorsen T, Maerkl SJ, Quake SR (2002) Microfluidic large-scale integration. Science 298:580–584. doi:10.1126/science.1076996

Unger MA, Chou H-P, Thorsen T et al (2000) Monolithic microfabricated valves and pumps by multilayer soft lithography. Science 288:113–116. doi:10.1126/science.288.5463.113

Verma MKS, Majumder A, Ghatak A (2006) Embedded template-assisted fabrication of complex microchannels in PDMS and design of a microfluidic adhesive. Langmuir 22:10291–10295. doi:10.1021/la062516n

Vijayendran RA, Motsegood KM, Beebe DJ, Leckband DE (2002) Evaluation of a three-dimensional micromixer in a surface-based biosensor. Langmuir 19:1824–1828. doi:10.1021/la0262250

Wheeler AR, Throndset WR, Whelan RJ et al (2003) Microfluidic device for single-cell analysis. Anal Chem 75:3581–3586

Wu H, Brittain S, Anderson J et al (2000) Fabrication of topologically complex three-dimensional microstructures: metallic microknots. J Am Chem Soc 122(51):12691–12699

Wu H, Odom TW, Chiu DT, Whitesides GM (2003) Fabrication of complex three-dimensional microchannel systems in PDMS. J Am Chem Soc 125:554–559. doi:10.1021/ja021045y

Wu H, Wheeler A, Zare RN (2004) Chemical cytometry on a picoliter-scale integrated microfluidic chip. Proc Natl Acad Sci USA 101:12809–12813. doi:10.1073/pnas.0405299101

Wu W, DeConinck A, Lewis JA (2011) Omnidirectional printing of 3D microvascular networks. Adv Mater 23:H178–H183. doi:10.1002/adma.201004625

Xia HM, Wan SYM, Shu C, Chew YT (2005) Chaotic micromixers using two-layer crossing channels to exhibit fast mixing at low Reynolds numbers. Lab Chip 5:748–755. doi:10.1039/b502031j

Xiong B, Ren K, Shu Y et al (2014) Recent developments in microfluidics for cell studies. Adv Mater 26:5525–5532. doi:10.1002/adma.201305348